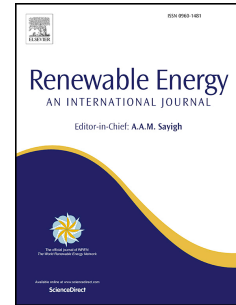


# Journal Pre-proof

A comparative study between racking systems for photovoltaic power systems

A. Barbón, P. Fortuny Ayuso, L. Bayón, C.A. Silva



PII: S0960-1481(21)01231-3

DOI: <https://doi.org/10.1016/j.renene.2021.08.065>

Reference: RENE 15876

To appear in: *Renewable Energy*

Received Date: 30 January 2021

Revised Date: 13 July 2021

Accepted Date: 18 August 2021

Please cite this article as: Barbón A, Ayuso PF, Bayón L, Silva CA, A comparative study between racking systems for photovoltaic power systems, *Renewable Energy* (2021), doi: <https://doi.org/10.1016/j.renene.2021.08.065>.

This is a PDF file of an article that has undergone enhancements after acceptance, such as the addition of a cover page and metadata, and formatting for readability, but it is not yet the definitive version of record. This version will undergo additional copyediting, typesetting and review before it is published in its final form, but we are providing this version to give early visibility of the article. Please note that, during the production process, errors may be discovered which could affect the content, and all legal disclaimers that apply to the journal pertain.

© 2021 Published by Elsevier Ltd.

**A. Barbón:** Conceptualization, Methodology

**P. Fortuny Ayuso:** Software, Methodology, Writing-Original draft preparation.

**L. Bayón:** Conceptualization, Methodology

**C. A. Silva:** Methodology, Data curation

Journal Pre-proof

# A comparative study between racking systems for photovoltaic power systems

A. Barbón<sup>a</sup>, P. Fortuny Ayuso<sup>b</sup>, L. Bayón<sup>b\*</sup>, C.A. Silva<sup>c</sup>

<sup>a</sup>Department of Electrical Engineering, University of Oviedo, Spain

<sup>b</sup>Department of Mathematics, University of Oviedo, Spain

<sup>c</sup>Center for Innovation, Technology and Policy Research –IN+, Instituto Superior Técnico, University of Lisbon, Portugal

\*Corresponding author: L. Bayón, email: bayon@uniovi.es

---

## Abstract

We present a comparative study of the different racking systems used in photovoltaic power systems, with a new methodology for determining the total energy produced by each one under usual weather conditions (not clear-skies). In systems without solar tracker, the tilt angle is a major factor contributing to the energy production, and its optimization is essential. We study the effect of tilt update frequency (daily, monthly, or constant) on the total irradiation received by a plane surface, and present a method for computing the optimal tilt angle, which we validate using previous studies. This method is easily implemented, accurate, and valid for any location. We compare all the systems with the most energy-productive one, the dual-axis tracker, in two ways: with respect to energy production, and to levelized cost of energy, both in 39 cities around the World. The results provide a new insight on the relative and objective value of trackerless systems, and some remarkable properties arise, which may be relevant in budgetary consideration.

---

1    **Keywords:** Photovoltaic Power Systems, Racking systems with solar  
2    tracker, Racking systems without solar tracker, Optimum Tilt Angle.

## 3    1. Introduction

4    In 2018, the global primary energy consumption grew by almost twice  
5    its 10-year average of 1.5% per year, with renewable energies accounting for  
6    the second largest increase [1], which forecasts an important reduction in the

7 dependence on fossil fuels. Solar energy, which is the main source of energy  
 8 on Earth [2] is the topic of our work, mainly photovoltaic power systems  
 9 (PVPS), their economic efficiency (see [3] for a survey), and applications. In  
 10 2018, about 103 (GW) of new PVPS was installed [4], and the total global  
 11 installed capacity of PV energy was around 512 (GW), 1.3 times what it was  
 12 in 2017 [4]. The economic efficiency is measured using the so-called levelized  
 13 cost of energy (LCOE), in USD/kWh. Its weighted average in 2018 was 0.085  
 14 (USD/kWh), and it is forecast to be between 0.02 and 0.08 (USD/kWh) by  
 15 2030, and between 0.014 and 0.05 (USD/kWh) by 2050 [5].

16 There are nowadays two kinds of racking systems used in PVPS: with,  
 17 and without solar tracker. Those with solar tracker are classified according  
 18 to their motion:

- 19 (i) With two axes of rotation (dual-axis trackers), which generate the  
 20 greatest amount of energy. They are adjusted in real time in order  
 21 to minimize the angle of incidence of the solar rays reaching its sur-  
 22 face. Two PV plants for power generation which use this system are:  
 23 the Ciurbesti Photovoltaic Park (1.0 MW) in Miroslava (Romania) [6],  
 24 and the plant at Yunnan (9 MW), China [7].
- 25 (ii) With a single axis of rotation, which can have different orientations:  
 26 horizontal North-South (named “single-axis trackers aligned with the  
 27 North-South axis”), horizontal East-West (named “single-axis trackers  
 28 aligned with the East-West axis”), or parallel to the Earth’s axis (named  
 29 “Polar axis trackers”). These have also real-time adjustment. In prac-  
 30 tice, the most used is the North-South aligned. Examples of PV plants  
 31 using this design are: CSF SEVILLA (39.984 MW) in Sevilla (Spain),  
 32 and Northern Light (141 MW) in Copiapó (Chile) (both with North-  
 33 South axis).

34 In racking systems without solar tracker, the PV modules have a fixed tilt  
 35 angle for a fixed period of time and are always South-oriented (in the North-  
 36 ern hemisphere). The tilt angle may be adjusted with different frequencies  
 37 (daily, monthly) or left constant, the latter being by far the most frequent  
 38 solution. Commercial PV plants for power generation using these systems  
 39 are: the Mohammed bin Rashid Al Maktoum Solar Park (613 MW) in Saih  
 40 Al-Dahal (United Arab Emirates) (constant tilt), and Telangana I (10 MW)  
 41 in Telangana (India) (Seasonal varying tilt angle) [7].

42 Although dual-axis trackers have the greatest total energy production,  
 43 they need not be optimal for a specific installation. Other factors to be taken  
 44 into account are: initial investment cost, required area for the installation,  
 45 soil conditions, topography...:

- 46 (i) *Initial investment cost.* Dual axis tracker systems are more expensive  
 47 to procure and install: they generally add a premium of 40 – 50% to  
 48 the average deployment costs with respect to a system of the same size  
 49 without solar tracker, and 20 – 25% with respect to a similarly-sized  
 50 single-axis tracker system [8]. The use and cost of land is not contained  
 51 as an input parameter.
- 52 (ii) *Soil condition.* Solar trackers add torque to the foundations of the  
 53 system, which may need to be larger and placed deeper, increasing  
 54 the cost of the civil work. Actually, the installation of trackers may be  
 55 prevented to all practical purposes if there is no shallow bedrock.
- 56 (iii) *Topography.* Solar trackers are only viable in relatively flat locations, so  
 57 much so that they cannot be installed in places with inclinations greater  
 58 than 15° [8]. Thus, previous to the installation, ground undulations  
 59 may need to be leveled to a certain tolerance. This may increase the  
 60 deployment cost and make them uneconomical [9].
- 61 (iv) *Expected lifespan.* Moving parts are one of the main drawbacks in this  
 62 respect. This makes trackerless systems optimal for very long lived  
 63 installations, and single-axis trackers better than dual-axis ones [8].
- 64 (v) *Operation and maintenance costs.* There is no standardized notion of  
 65 annual operation and maintenance cost [10]. However, according to  
 66 [11], a reasonable expectation for these annual costs of PV systems is  
 67 around 0.5% and 1% of the initial investment for large and for small  
 68 systems, respectively.
- 69 (vi) *Wind loads.* When the wind speed is greater than 70 km/h [8], systems  
 70 with solar tracker turn to their safety position. In it, the solar irradi-  
 71 ance absorbed by the system is very low compared to the optimal one.  
 72 Obviously, trackless systems have not this problem.

73 All the above factors influence the installation of a PV system with or  
 74 without trackers. In this paper, our analysis will also cover trackless systems

75 whose tilt can be updated at different frequencies, as explained above (daily,  
 76 monthly...). In order to make an informed assessment prior to deployment,  
 77 one needs to have a good forecast of the total energy produced by the system,  
 78 using different tracking methods. This comparison is the aim of this paper.

79 From the point of view of efficiency (both energetic and budgetary), the  
 80 installation angles of a racking systems without solar tracker are key. The  
 81 two main angles are: tilt and surface azimuth. The tilt angle ( $\beta$ ) is the  
 82 angle between the plane of the surface and the horizontal plane. The surface  
 83 azimuth angle ( $\gamma$ ) is the angle between the projection on a horizontal plane  
 84 of the normal to the tilted surface and the geographical South (East being  
 85 negative and West positive). The optimum surface azimuth angle for these  
 86 systems is, usually, in the northern hemisphere,  $\gamma_{opt} = 0^\circ$  (In the southern  
 87 hemisphere,  $\gamma_{opt} = 180^\circ$ ) [12], so that it requires no discussion. For its part,  
 88 the tilt angle  $\beta$  is a critical parameter, and knowledge of its optimum provides  
 89 a great economic benefit. Some factors which influence the value of this  
 90 optimum are, among others: (1) the period during which  $\beta$  is constant, which  
 91 can vary from minutes to the whole year, (2) the location of the installation:  
 92 ground, roof, balcony... (3) the latitude of the place, (4) weather conditions,  
 93 (5) climatic conditions (polluted air, snow fall, dust storms).

94 Numerous papers study the optimum tilt angle of racking systems without  
 95 solar tracker with constant tilt, at different sites throughout the World [13],  
 96 [14]. Their models differ in simplicity of use and accuracy. Roughly speaking,  
 97 these models can be grouped in two categories: those based on the latitude,  
 98 in which the optimal tilt angle is taken as the latitude plus or minus a specific  
 99 value obtained via analytic methods (v.gr. regression analysis), and those  
 100 who try to maximize the total irradiation falling onto the tilted surface.  
 101 The former are very simple but prone to error, while the latter, generally  
 102 more accurate, depend strongly (for their accuracy) on the model of solar  
 103 irradiance they use; furthermore, their utilization is more complex.

104 Assuming that the installation of one of these systems is South oriented,  
 105 Jiménez et al. [15] suggest that the optimum tilt angle (constant throughout  
 106 the year) is  $\beta_{opt} = \lambda - 10.38^\circ$  for Barcelona (Spain) (whose latitude is  $\lambda =$   
 107  $41.38^\circ$ ) and  $\beta_{opt} = \lambda - 8.77^\circ$  for Jaen (Spain) ( $\lambda = 37.77^\circ$ ). Darhmaoui et  
 108 al. [16] obtained  $\beta_{opt} = \lambda - 2.06^\circ$  for Lyon (France) ( $\lambda = 45.76^\circ$ ). They, and  
 109 other authors, also present other optimum tilt angles for places around the  
 110 world [16, 17]. The seek for a formula for the optimum tilt angle depending on  
 111 the latitude is an active area of research. The hemisphere is usually divided  
 112 into two halves:  $\lambda < 45^\circ$  and  $\lambda \geq 45^\circ$  [18]. For locations with  $\lambda < 45^\circ$ , one

113 of the most used formulas appears in [19]:  $\beta_{opt} = 3.7 + 0.69 \cdot |\lambda|$ , whereas for  
 114  $\lambda > 45^\circ$ , [18] gives:  $\beta_{opt} = (3.7 + 0.69 \cdot |\lambda|) - 10^\circ$ . However, in [20] the division  
 115 is made at  $\lambda = 65^\circ$ , giving, for  $\lambda < 65^\circ$ , the formula  $\beta_{opt} = 2.14 + 0.764 \cdot \lambda$ ,  
 116 and for  $\lambda \geq 65^\circ$ ,  $\beta_{opt} = 33.65 + 0.224 \cdot \lambda$ . Talebizadeh et al. [21] give a  
 117 general linear formula:  $\beta_{opt} = 7.203 + 0.6804 \cdot \lambda$ , and finally, Jacobson [22]  
 118 provides a 3rd degree polynomial:  $\beta_{opt} = 1.3793 + \lambda(1.2011 + \lambda(-0.014404 +$   
 119  $0.000080509\lambda))$ . The accuracy of these formulas depends considerably on  
 120 the assumption of clear skies (no cloud cover) throughout the year. This is  
 121 especially significant for countries located above  $45^\circ N$ , most of which have  
 122 long seasons of cloudiness. Frequently, non-optimal tilt angles are used in  
 123 installations. For instance, increasing the number of PV modules may be  
 124 better than just collecting the maximum energy per module (e.gr. a greater  
 125 tilt angle may allow to install more modules in the same area[23]).

126 There are also many location-specific studies, which mix theoretical con-  
 127 siderations, irradiation models and software products to compute the opti-  
 128 mum  $\beta$ . For instance (and not intending to be exhaustive), Ullah et al [24]  
 129 use a solar irradiation transposition model, data from the National Renew-  
 130 able Energy Laboratory (NREL) [25] and the Energy Sector Management  
 131 Assistance Program (ESMAP) [26] to compute that optimum for a site in  
 132 Pakistan. Lv et al. [27] do the same for Lhasa (China), proposing the concept  
 133 of effective solar heat collection, and using data from the Meteorological Data  
 134 Set for China Building Thermal Environment Analysis [28]. Jafarkazemi et  
 135 al. [29] use experimental data for different orientations ( $0^\circ \leq \gamma \leq 90^\circ$ ) and  
 136 tilt angles ( $0^\circ \leq \beta \leq 90^\circ$ ) and data from the NASA Surface Meteorology  
 137 and Solar-Energy model [30]. Skeiker [31] provides a mathematical model for  
 138 determining the optimum  $\beta$  in several places in Syria, based on maximizing  
 139 the extraterrestrial solar radiation for a specific date or period. Nafeh [32],  
 140 on its part, maximizes the incident solar irradiance at solar noon on a PV  
 141 array, for each day, month or year. MATLAB code is used in [24], [27], [29]  
 142 for their computations.

143 Racking systems without solar tracker with monthly tilt update are scar-  
 144 cely studied: [24, 33, 34] are some references, but we have found no studies  
 145 of these systems using daily tilt updates.

146 In summary, for racking systems without solar tracker, the present situ-  
 147 ation is as follows: there are studies for specific locations (which cannot be  
 148 used elsewhere) and there are formulas whose accuracy depends greatly on  
 149 the weather and climate conditions of the site (so, they are useful but not  
 150 too precise).

151 The present study aims to compare the total energy obtained and the  
 152 levelized cost of the produced electrical energy (LCOE) for the racking sys-  
 153 tems used in PVPS. For racking systems with solar tracker, we shall use the  
 154 equations proposed in [12]. For those without solar tracker, we study three  
 155 update frequencies of the tilt angle  $\beta$ : daily, monthly, and constant. Our an-  
 156 alytical procedure uses an algorithm which maximizes the solar irradiation  
 157 reaching the tilted surface for a given period of time, providing the opti-  
 158 mum tilt angles for each day/month/whole year (depending on the update  
 159 frequency). As a matter of fact, it can be applied to any update frequency  
 160 (for instance, a different angle depending only on the hot/cold or dry/humid  
 161 seasons). This analytical procedure is designed to obtain formulae which re-  
 162 quire the least number of parameters to determine optimum tilt angles. Our  
 163 analysis is performed for 39 locations covering all the populated latitudes in  
 164 the Northern Hemisphere and a large spectrum of longitudes.

165 The paper is organized as follows: the geographic characteristics of the  
 166 cities under study are presented in Section 2. The proposed methodology is  
 167 described and validated in Section 3; also in this section, the total (annual)  
 168 energy obtained for each racking system and the valuation indicators are  
 169 provided. Section 4 presents the results of the study. Finally, Section 5  
 170 summarizes the main contributions and conclusions of the paper.

## 171 2. Case study

172 In order to obtain a thorough assessment of the comparison by tilt update  
 173 frequency across the World, we have selected 39 cities between  $6^\circ$  and  $60^\circ$   
 174 latitude North, covering a wide range of longitudes. We focus on the Northern  
 175 hemisphere for two reasons: 90% of the World population lives in it [35] and  
 176 it contains 60% of the Earth's available land. These locations are given in  
 177 Table 1, together with their main geographical characteristics.

## 178 3. Methodology

179 We use the following procedure: first, the solar irradiance at a specific  
 180 latitude is estimated using the model proposed by [36]. Then, we estimate  
 181 the amount of total irradiation reaching a tilted plane using a method de-  
 182 rived from [12]. We then proceed to compute the optimum tilt angle of a  
 183 racking system without solar tracker with different update frequencies (daily,

Table 1. Cities under study.

Id	City	Latitude	Longitude	Alt.(m)
1	Medellin (CO)	06°14'38"N	75°34'04"W	1469
2	Colombo (LK)	06°56'06"N	79°51'14" E	8
3	Bangkok (TH)	13°45'14"N	100°29'34" E	9
4	Dakar (SN)	14°41'34"N	17°26'52"W	12
5	Morelia (MX)	19°42'10"N	101°11'24"W	1921
6	El Paso (MX)	21°08'42"N	21°08'42"W	192
7	Karachi (PK)	24°52'01"N	67°01'51" E	14
8	Delhi (IN)	28°39'07"N	77°13'19"W	224
9	New Orleans (US)	29°57'00"N	90°04'12"W	40
10	Cairo (EG)	30°29'24"N	31°14'38"W	41
11	Hefei (CN)	31°45'07"N	117°19'55" E	10
12	Djelfa (DZ)	34°20'34"N	03°16'15" E	1011
13	Albuquerque (US)	35°05'02"N	35°05'02"W	1519
14	Handan (CN)	36°06'42"N	114°29'22" E	71
15	Desert Rock (US)	36°37'00"N	97°43'37"W	1007
16	Almeria (ES)	36°50'07"N	02°24'08"W	22
17	Madrid (ES)	40°25'01"N	03°42'14"W	665
18	New York (US)	40°42'46"N	74°00'21"W	26
19	Rock Springs (US)	40°43'00"N	77°51'32"W	376
20	Chicago (US)	41°51'00"N	87°39'00"W	180
21	Rome (IT)	41°53'30"N	12°30'40" E	52
22	Toronto (CA)	43°39'14"N	79°23'13"W	106
23	San Marino (IT)	43°56'45"N	12°27'28" E	363
24	Olympia (US)	47°02'42"N	122°53'42"W	2
25	Nantes (FR)	47°13'08"N	01°33'14"W	16
26	Budapest (HU)	47°29'52"N	19°02'23" E	111
27	Seattle (US)	47°36'22"N	122°19'55"W	56
28	Freiburg (DE)	47°59'45"N	07°50'56" E	282
29	Wien (AT)	48°15'00"N	16°21'00" E	203
30	Valentia (IE)	51°48'00"N	10°14'38"W	14
31	Saskatoon (CA)	52°07'56"N	106°40'08"W	454
32	Quebec (CA)	52°28'33"N	71°49'33"W	477
33	Berlin (DE)	52°31'27"N	13°24'37" E	37
34	Hamburg (DE)	53°33'00"N	10°00'03" E	19
35	Alberta (CA)	55°00'03"N	115°00'07"W	1045
36	Tartu (EE)	58°15'00"N	26°43'48" E	70
37	S. Petersburg (RU)	59°56'20"N	30°18'57" E	14
38	Lerwick (GB)	60°08'00"N	01°08'55"W	63
39	Helsinki (FI)	60°10'10"N	24°56'07" E	23

184 monthly, and constant) using a novel method which we describe. The val-  
 185 idation of this method is performed by comparing it to other procedures  
 186 proposed in the literature. The equations providing the optimal tilts for  
 187 each type of racking system with solar tracker are then presented, and, using  
 188 the irradiances obtained in the first two steps, the values of total annual  
 189 irradiation ( $\text{MWh}/\text{m}^2$ ) are estimated for systems with trackers. Finally, we  
 190 provide a detailed comparative study of LCOE for all the systems.

### 191 3.1. Step 1. Model for estimating the solar irradiance

192 The total annual solar irradiation depends strongly on the geography and  
 193 weather conditions of the site. In order to get a good estimation, one needs  
 194 accurate site-specific data. The most common measurements in ground-level  
 195 meteorological stations are the global and diffuse solar irradiances on a hori-  
 196 zontal surface. Absent these values, one can only rely on theoretical estima-  
 197 tions from irradiance models, and thus only approximate optimal values for  
 198 the tilt can be expected.

199 Theoretical models for computing each component of the solar irradiance  
 200 are manifold, and their accuracy differs by latitude [17]. One might cite the  
 201 clear sky models of [37], satellite estimations [38], Angström's sunshine hours  
 202 method [39], methods based on temperature records [40]...

203 In this work, we use the method presented in [36] to determine the hourly  
 204 beam and diffuse horizontal solar irradiances. It takes into account the site's  
 205 weather conditions for each day of the year. Using Hottel's model [41] for  
 206 estimating the beam solar irradiance transmitted through clear atmospheres,  
 207 Liu and Jordan's model [42] for determining diffuse solar irradiance for clear-  
 208 sky, and Fourier series approximation for correcting those clear-sky models,  
 209 it adapts them to the climatological conditions of the specific location. It  
 210 has been validated for different climates, against actual data obtained from  
 211 ground-level stations (the WRDC database [43]). For instance, in Wien (Aus-  
 212 tria), a place which we also cover in this paper, the  $R^2$  coefficient for daily  
 213 beam irradiation is 0.85713, and for daily diffuse irradiation it is 0.948112  
 214 (values which are generally considered proof of a very good fit [44]).

### 215 3.2. Step 2. Estimation of the amount of total irradiation on a tilted plane

216 The total solar irradiance ( $I_t$ ) on a tilted surface is usually calculated  
 217 as the sum of three components: the beam ( $I_{bt}$ ), the diffuse ( $I_{dt}$ ), and the  
 218 ground reflected ( $I_{rt}$ ) irradiances. The beam and reflected components are  
 219 always computed the same way (using geometric considerations for the former

220 and isotropic models for the latter), while there are multiple methods for  
 221 the diffuse component. As the surface is tilted, and the irradiance is time-  
 222 dependent, the following parameters are relevant: tilt angle, surface azimuth  
 223 angle, and incident angle of the Sun.

224 Specifically: the *beam irradiance* is the component of the total irradiance  
 225 which is received from the Sun without atmospheric scattering [12]; it can be  
 226 estimated from the geometric relation between the horizontal plane and the  
 227 tilted surface.

228 The *ground-reflected irradiance* is the fraction of the total irradiance re-  
 229 flected by the surface of the Earth and by any other surface (buildings, trees,  
 230 etc.). It is essentially impossible to compute exactly, due to the many factors  
 231 contributing to it [12]. However, one can assume [12, 45], that the reflec-  
 232 tion on the ground of the beam and diffuse solar irradiances is isotropic. At  
 233 the same time, it is also usually assumed [20] that the surroundings of the  
 234 tilted surface have a constant diffuse reflectance, called ground reflectance  
 235 ( $\rho_g$ ), which depends on the type of ground surrounding the tilted surface.  
 236 Muneer [46] computed its value for small surfaces. For instance, for weath-  
 237 ered concrete  $\rho_g = 0.22$ ; for dark surfaces of buildings (red brick, dark paints,  
 238 etc.)  $\rho_g = 0.27$ ; and for light surfaces of buildings (light brick, light paints,  
 239 etc.)  $\rho_g = 0.60$ . For green vegetation and some soil types, one usually takes  
 240  $\rho_g = 0.20$ .

241 The *diffuse irradiance* is the component of the irradiance which has suf-  
 242 fered scattering [12], so that its direction is hard to determine; it is divided  
 243 into three components: isotropic, circumsolar and horizon brightening irradi-  
 244 ances. The first one is received evenly from the entire sky dome. The second  
 245 one is concentrated in the section of the sky around the Sun, whereas the  
 246 last one is concentrated near the horizon and is most obvious in clear skies  
 247 [47]. The models used to predict this solar irradiance on a tilted surface can  
 248 be grouped in two families: isotropic and anisotropic.

- 249 (i) The isotropic models assume, as their name suggests, that the diffuse  
 250 irradiance is only isotropic [45, 48, 49, 50], so that it only depends on  
 251 the tilt angle  $\beta$  of the surface.
- 252 (ii) Some anisotropic models assume that it is composed of an isotropic  
 253 and a circumsolar component only [51, 52, 53], [54], [55]. They depend  
 254 mainly on  $\beta$ , the Sun height  $\alpha_S$ , and the incidence angle  $\theta_i$ , apart from  
 255 other model-related parameters.

256 (iii) There are other anisotropic models in which it is assumed composed  
 257 of an isotropic, a circumsolar, and a horizon brightening component  
 258 [56, 57, 58]. They also depend on  $\beta$ ,  $\alpha_S$ ,  $\theta_i$ , and other model-related  
 259 parameters.

260 Mehleri et al. [59] have compared several isotropic [45, 48, 49, 50] and  
 261 anisotropic models [51, 52, 53, 56, 57, 58, 60]. They conclude that the most  
 262 accurate results were produced with the Liu and Jordan model [45]. Hence, it  
 263 is commonly recommended for forecasting the diffuse irradiance at locations  
 264 throughout the world [47, 12, 61].

265 The total irradiance  $I_t(n, T, \beta)$  depends on the tilt angle  $\beta$ , the day of the  
 266 year  $n$  and the solar time  $T$ , and is computed as:

$$267 \quad I_t(n, T, \beta) = I_{bh}(n, T) \cdot \frac{\cos \theta_i}{\cos \theta_z} + I_{dh}(n, T) \cdot \left( \frac{1 + \cos \beta}{2} \right) +$$

$$(I_{bh}(n, T) + I_{dh}(n, T)) \cdot \rho_g \cdot \left( \frac{1 - \cos \beta}{2} \right) \quad (1)$$

where  $I_{bh}$  (W/m<sup>2</sup>) is the beam irradiance on a horizontal plane,  $\theta_z$  (°) is the  
 zenith angle of the sun,  $\theta_i$  (°) is the incident angle,  $I_{dh}$  (W/m<sup>2</sup>) is the diffuse  
 irradiance on a horizontal plane,  $\beta$  (°) is the tilt angle, and  $\rho_g$  (dimension-  
 less) is the ground reflectance. Solar time is the time used in the sun-angle  
 relations, and in this work we set the time variable to mean Solar time. The  
 incident angle of the Sun  $\theta_i$  (°) on a tilted surface can be determined follow-  
 ing [12] as (notice that in all our formulas we assume the azimuth angle to  
 be  $\gamma = 0$ ):

$$\theta_i = \sin \delta \cdot \sin \lambda \cdot \cos \beta - \sin \delta \cdot \cos \lambda \cdot \sin \beta + \cos \delta \cdot \cos \lambda \cdot \cos \beta \cdot \cos \omega$$

$$+ \cos \delta \cdot \sin \lambda \cdot \sin \beta \cdot \cos \omega \quad (2)$$

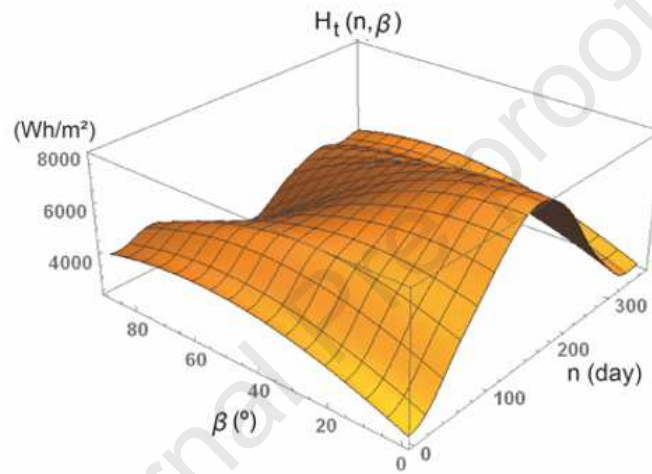
268 where  $\delta$  is the declination,  $\lambda$  the latitude,  $\beta$  the tilt angle, and  $\omega$  the hour  
 269 angle. When using equation (2), it is necessary to take into account that the  
 270 incidence angle might exceed 90° (i.e. the Sun is behind the surface and the  
 271 Earth is not blocking the Sun).

272 Using *eq.* (1), we can compute, by direct integration from sunrise to  
 273 sunset, the total irradiation on a tilted surface  $H_t(n, \beta)$  (Wh/m<sup>2</sup>) for each  $n$   
 274 day of the year, and each tilt angle  $\beta$  (where  $T_R(n)$  is the sunrise time and  
 275  $T_S(n)$  the sunset):

$$276 \quad H_t(n, \beta) = \int_{T_R(n)}^{T_S(n)} I_t(n, T, \beta) dT \quad (3)$$

277 This function  $H_t(n, \beta)$  is what allows us to compute the total annual irradiation on a tilted plane depending on the tilt settings.  
 278

279 It is at this point that a discretization of the tilt angle is necessary. We  
 280 have divided the range  $[0, 90]$  ( $^\circ$ ) into 900 intervals of width  $0.1$  ( $^\circ$ ). The 2-  
 281 variable function  $H_t(n, \beta)$  ( $\text{Wh}/\text{m}^2$ ) for the case of Almeria ((16), Spain, with  
 282 latitude  $36^\circ 50' 07''\text{N}$ , longitude  $02^\circ 24' 08''\text{W}$  and altitude  $22$  (m)) is shown in  
 283 Fig. 1.



284 Fig. 1. Total daily solar irradiation on a tilted surface  $H_t(n, \beta)$ .

### 285 3.3. Step 3. Determination of the optimum tilt angle for racking systems 286 without solar tracker

287 We now compute the total irradiation on a racking system without solar  
 288 tracker, for different update frequencies. We consider, in what follows, 3  
 289 different frequencies: (1) Daily, (2) Monthly, and (3) Yearly (constant tilt).

#### 290 3.3.1. Daily tilt updates

291 In the analytical procedure we propose, we assume in this step that the  
 292 tilt of the PV system is updated daily. Our method requires computing, for  
 293 each day  $n$ , the optimal tilt angle  $\beta$ , which we shall call  $\beta_{opt}^d(n)$ . Consider,  
 294 in Fig.1, each section of the surface  $H_t^n(\beta)$  for a fixed  $n$  (i.e. the function of  
 295 the variable  $\beta$  which gives the total solar irradiation for that day  $n$  if the tilt  
 296 angle is  $\beta$ ). We need to find, for that section, the tilt angle  $\beta_{opt}^d(n)$  such that  
 297 irradiation for that day:

$$298 \quad H_t^n(\beta_{opt}^d(n)) = \max_{\beta} H_t^n(\beta) \quad (4)$$

299 In some sense, we are finding the “crest” point for each  $n$  of the function  
 300  $H_t(n, \beta)$ . In Fig. 2 we show how  $\beta_{opt}^d$  varies throughout the year for our  
 301 chosen location (nr. 16, Almeria), and in Fig. 3 we plot the “crest” of values  
 302 of  $H_t(n, \beta)$  over those optima. The area under this crest is the maximum  
 303 energy than can be produced during a year when the tilt is modified daily.

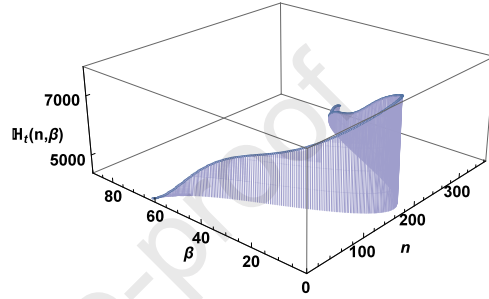


Fig. 2. Plot of  $\beta_{opt}^d(n)$ .

Fig. 3. Plot of  $H_t(n, \beta_{opt}^d(n))$ .

305 The shaded area in Fig. 3 (maximum energy under daily update of  $\beta$ ) is,  
 306 for Almeria (Spain):

$$307 \int_1^{365} H_t(n, \beta_{opt}^d(n)) dn = 2.22145 \times 10^6 \text{ (Wh/m}^2\text{)} \quad (5)$$

308 The validation of the proposed method is done comparing our results to those  
 309 obtained using the well-know formula of Duffie [12] for East-West trackers  
 310 with daily update. Notice, by the way, that in this case, Duffie’s formula  
 311 requires the azimuth  $\gamma$  of the receiver to change: it must be  $0^\circ$  if  $|\lambda - \delta| > 0$   
 312 and  $180^\circ$  if  $|\lambda - \delta| \leq 0$ ,  $\delta$  being the declination. Duffie’s daily formula is  
 313 given then by:

$$314 \beta_{opt} = |\lambda - \delta| \quad (6)$$

315 Table 2 contains the values of total annual irradiation ( $\text{MWh/m}^2$ ) estimated  
 316 using Duffie’s formula with daily update ( $H_{Duffie}^d$ ) and the proposed method  
 317 ( $H_{proposed}^d$ ).

318 The difference ratio in total annual irradiation with daily update is plotted  
 319 in Fig. 4. Notice that, in what follows, we shall refer to each city by their  
 320 Id number (first column of Table 1). The values are % with respect to the  
 321 Duffie’s method, that is:

$$322 \frac{H_{proposed}^d - H_{Duffie}^d}{H_{Duffie}^d} \cdot 100 \quad (7)$$

Table 2. Estimated total annual irradiation with daily update (MWh/m<sup>2</sup>).

City	Duffie	Proposed	City	Duffie	Prop.	City	Duffie	Prop.
Medellin	1.8947	1.8953	Handan	1.5516	1.5620	Seattle	1.4199	1.4319
Colombo	2.0977	2.0989	Desert Rock	2.4620	2.4743	Freiburg	1.4287	1.4396
Bangkok	1.9543	1.9558	Almeria	2.2127	2.2214	Wien	1.3746	1.3886
Dakar	2.3006	2.3038	Madrid	1.9696	1.9806	Valentia	1.0721	1.0907
Morelia	2.2865	2.2931	New York	1.6480	1.6575	Saskatoon	1.4449	1.4585
El Paso	1.8150	1.8178	Rock Springs	1.4717	1.4819	Quebec	1.1933	1.2091
Karachi	2.3433	2.3477	Chicago	1.5843	1.5950	Berlin	1.2026	1.2212
Delhi	2.0695	2.0751	Rome	1.8636	1.8737	Hamburg	1.1981	1.2115
New OrL.	1.9035	1.9096	Toronto	1.4901	1.5018	Alberta	1.3638	1.3799
Cairo	2.3859	2.3939	San Marino	1.5954	1.6080	Tartu	1.0698	1.0890
Hefei	1.4332	1.4420	Olympia	1.3562	1.3687	S. Peters.	1.1369	1.1530
Djelfa	2.2755	2.2864	Nantes	1.5015	1.5121	Lerwick	0.8429	0.8666
Alburq.	2.3844	2.3969	Budapest	1.2980	1.3145	Helsinki	1.0724	1.0899

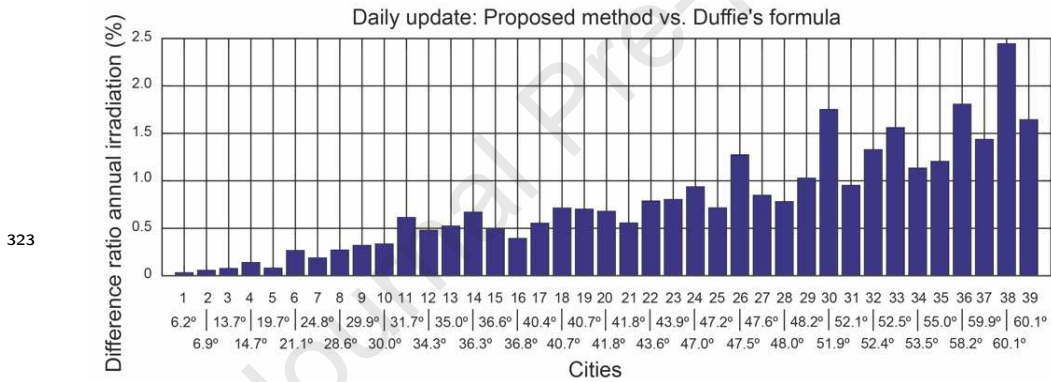


Fig. 4. Difference ratio of total annual irradiation between proposed daily update and Duffie's formula.

324 Comparing our method with Duffie's daily method (6), using Fig. 4, we  
 325 can conclude (apart from our method being consistently better than Duffie's):

- 326 (i) The present model can be considered validated, as these deviations are  
 327 not greater than 2.5%.
- 328 (ii) For locations with  $\lambda < 45^\circ$ , the improvement is slight: between 0.03%  
 329 and 0.79%.
- 330 (iii) However, when  $\lambda > 45^\circ$ , the improvements are larger, up to 2.44% in  
 331 Lerwick (nr. 38).

332 In order to try and explain this improvement, we have plotted, in Fig.  
 333 5, the daily values of  $\beta_{opt}^d$  (proposed method) and Duffie's daily optimum  
 334 tilts, in the case of Almeria (nr. 16). Notice the remarkable difference from  
 335 the Spring to the Autumn equinox, where our method (because it takes into  
 336 account the meteorological conditions) suggests a decrease in the tilt angle  
 337 with respect to Duffie's: Almeria is one of the sunniest places in Europe. In  
 338 other places, a similar behavior is noticeable, although the major difference  
 339 may take place at other times (Spring, Winter...), and the optimum tilt angle  
 340 is adjusted according to the climatic and weather conditions of each location.

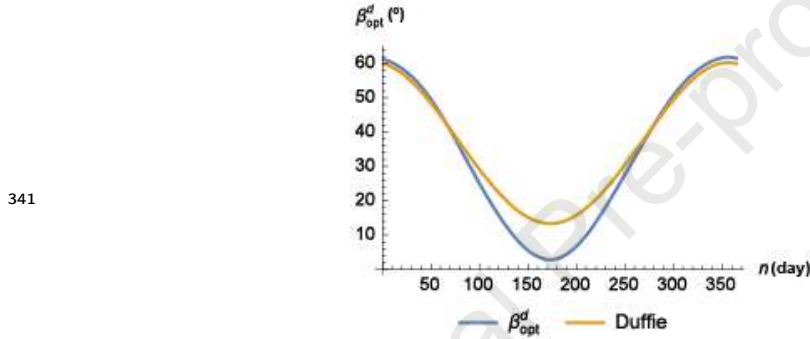


Fig. 5. Daily values of  $\beta_{opt}^d(n)$  and Duffie's formula (6).

### 342 3.3.2. Monthly tilt updates

343 We now consider, in our analytical method, a PV system whose tilt angle  
 344 is modified monthly. We have to divide the period into the 12 months and  
 345 solve as many optimization problems of the form:

$$346 \quad H_t^{\beta,m} = \int_{f(m)}^{l(m)} H_t(n, \beta) dn; \quad \max_{\beta} H_t^{\beta,m}; \quad m = 1, \dots, 12 \quad (8)$$

347 where  $f(m)$  and  $l(m)$  are the first and last days of each month, respectively.  
 348 Calling  $\beta_{opt}^m(m)$  the optimum  $\beta$  for each month  $m$ , we obtain, for Almeria  
 349 (nr. 16), the 12 values (in degrees):

$$350 \quad \beta_{opt}^m(m) = [59.1, 51.0, 37.9, 22.4, 9.8, 3.5, 6.4, 17.3, 31.7, 46.0, 56.6, 61.4] \quad (9)$$

351 and the maximum annual irradiation is now:

$$352 \quad \sum_{m=1}^{12} \max_{\beta} H_t^{\beta,m} = 2.21878 \times 10^6 \text{ (Wh/m}^2\text{)} \quad (10)$$

Table 3. Estimated annual irradiation, monthly tilt updates (MWh/m<sup>2</sup>).

City	Irrad.	City	Irrad.	City	Irrad.
Medellin	1.8940	Handan	1.5606	Seattle	1.4303
Colombo	2.0971	Desert Rock	2.4708	Freiburg	1.4380
Bangkok	1.9543	Almeria	2.2188	Wien	1.3871
Dakar	2.3015	Madrid	1.9783	Valentia	1.0896
Morelia	2.2906	New York	1.6557	Saskatoon	1.4566
El Paso	1.8165	Rock Springs	1.4804	Quebec	1.2076
Karachi	2.3453	Chicago	1.5933	Berlin	1.2200
Delhi	2.0729	Rome	1.8717	Hamburg	1.2102
New Orleans	1.9075	Toronto	1.5002	Alberta	1.3780
Cairo	2.3913	San Marino	1.6063	Tartu	1.0878
Hefei	1.4410	Olympia	1.3673	S. Petersburg	1.1517
Djelfa	2.2836	Nantes	1.5103	Lerwick	0.8656
Albuquerque	2.3936	Budapest	1.3133	Helsinki	1.0885

353 Table 3 contains the values of total annual irradiation (MWh/m<sup>2</sup>) estimated  
 354 using the proposed method with monthly update.

### 355 3.3.3. Constant tilt (year-long optimization)

356 Finally, we consider that the tilt angle of the PV system is constant.  
 357 When this happens (so that, most likely, the PV system is totally rigid), the  
 358 volume underneath the graph of our two-variable function is given by the  
 359 double integral

$$360 \iint_D H_t(n, \beta) \, dn d\beta \quad (11)$$

361 where  $D$  is the rectangle  $D : [1, 365] \times [0, 90]$ . In what follows, the reader  
 362 will notice that our method is essentially, the application of Cavalieri's prin-  
 363 ciple of integral calculus, whose proper generalization is Fubini's Theorem  
 364 [62]. In order to compute the optimal year-long constant tilt  $\beta_{opt}$ , we dis-  
 365 cretise the interval  $[0, 90]$  as above and compute the integral for each of the  
 366 values provided by that discretization. Following the Cavalieri idea, we are  
 367 evaluating:

$$368 H_t^\beta = \int_1^{365} H_t(n, \beta) \, dn \quad (12)$$

369 And we seek  $\beta_{opt}^y$  such that:

$$370 \quad H_t^{\beta_{opt}^y} = \max_{\beta} H_t^{\beta} \quad (13)$$

371 just by exhaustive search. In order to clarify the exposition, we show again  
 372 the case of Almeria (nr. 16). Fig. 6 contains the plot of  $H_t^{\beta}$  against  $\beta$ :  
 373 there is a clear maximum near  $30^\circ$ , which for a discretization in tenths of  
 374 angle, is actually  $\beta_{opt}^y = 30.3^\circ$ . In Fig. 7 we plot  $H_t(n, \beta)$  only for this  
 375 specific value  $\beta = \beta_{opt}^y$ . The shaded area represents the maximum possible  
 376 total annual irradiation with a fixed tilt. For this value of  $\beta_{opt}^y$ , we obtain  
 377  $\max_{\beta} H_t^{\beta} = 2.1084 \cdot 10^6$  (Wh/m<sup>2</sup>).

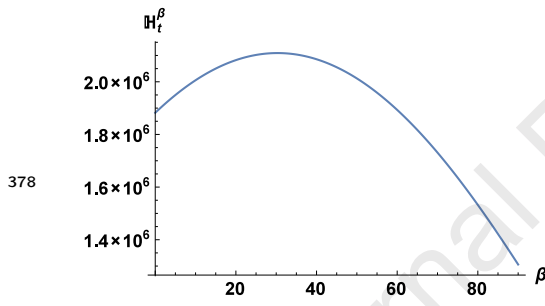


Fig. 6. Plot of  $H_t^{\beta}$ .

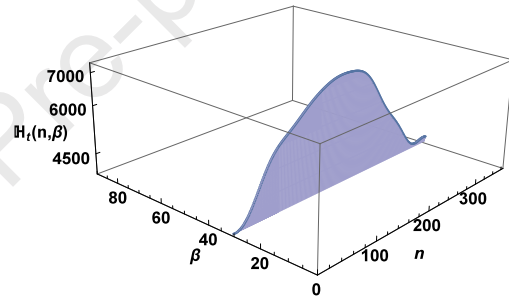


Fig. 7. Annual irradiation for  $\beta_{opt}^y$ .

379 There exist multiple elementary formulas for computing the tilt angle as  
 380 rule of thumb by solar energy system installers [18, 19, 20, 21]. However,  
 381 the validation of the proposed method is done using Jacobson's formula [22],  
 382 which is better than a simple linear interpolation. As a matter of fact,  
 383 Jacobson's model is considered a good fit for real-life PV systems [63], and  
 384 it has been used extensively [64, 65, 66]. Jacobson's formula for a constant  
 385 optimum tilt angle depending on the latitude  $\lambda$  is [22]:

$$386 \quad \beta_{opt} = 1.3793 + \lambda(1.2011 + \lambda(-0.014404 + 0.000080509\lambda)) \quad (14)$$

387 Fig. 8 shows the annual (i.e. constant) optimum tilt angle  $\beta_{opt}^y$  (proposed  
 388 method) for the 39 cities and the one computed using Jacobson's formula,  
 389 Eq. (14) [22].

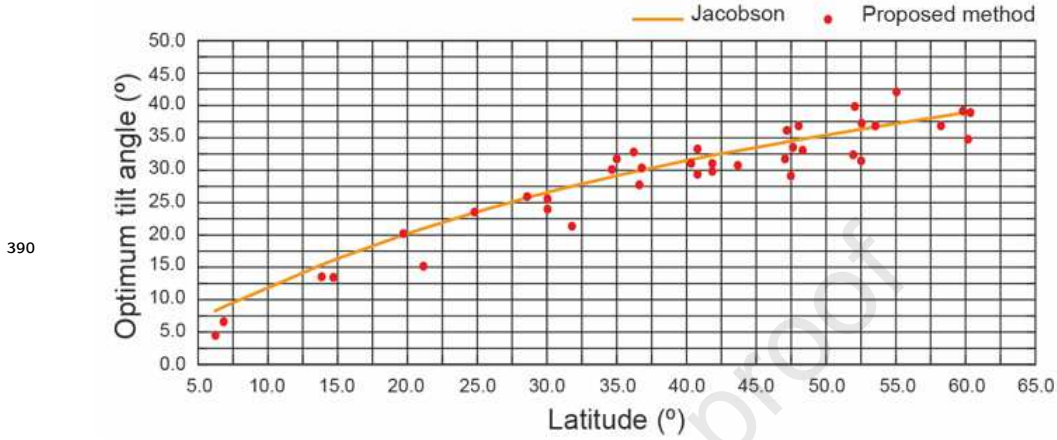


Fig. 8. Optimum tilt angle for cities under study and Jacobson's formula.

391 Table 4 contains the values of total annual irradiation ( $\text{MWh}/\text{m}^2$ ) esti-  
 392 mated using Jacobson's formula ( $H_{Jacobson}^y$ ) and with the proposed method  
 393 ( $H_{proposed}^y$ ). The difference ratio in total annual irradiation with constant tilt  
 394 is shown in Fig. 9. The values are %, with respect to the Jacobson's method,  
 395 that is:

$$396 \frac{H_{proposed}^y - H_{Jacobson}^y}{H_{Jacobson}^y} \cdot 100 \quad (15)$$

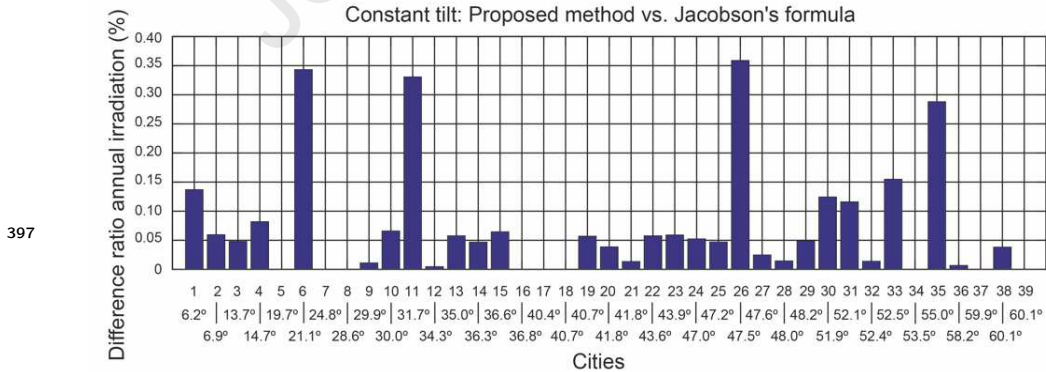


Fig. 9. Difference ratio in total annual irradiation with constant tilt:  
 proposed method vs. Jacobson's formula.

398 From Figs. 8 and 9 we can easily conclude:

Table 4. Estimated annual irradiation, Jacobson and fixed (constant) tilt (MWh/m<sup>2</sup>).

City	Jacob.	Fixed	City	Jacob.	Fixed	City	Jacob.	Fixed
Medellin	1.8274	1.8299	Handan	1.4992	1.4999	Seattle	1.3777	1.3779
Colombo	2.0197	2.0209	Desert Rock	2.3276	2.3291	Freiburg	1.3796	1.3799
Bangkok	1.8843	1.8852	Almeria	2.1084	2.1084	Wien	1.3403	1.3408
Dakar	2.2001	2.2019	Madrid	1.8889	1.8891	Valentia	1.0533	1.0547
Morelia	2.1772	2.1772	New York	1.5816	1.5817	Saskatoon	1.3887	1.3901
El Paso	1.7487	1.7547	Rock Spr.	1.4209	1.4217	Quebec	1.1566	1.1567
Karachi	2.2398	2.2398	Chicago	1.5305	1.5312	Berlin	1.1886	1.1907
Delhi	1.9881	1.9881	Rome	1.7954	1.7958	Hamburg	1.1701	1.1701
New OrL.	1.8217	1.8219	Toronto	1.4442	1.4450	Alberta	1.3060	1.3095
Cairo	2.2764	2.2779	San Marino	1.5438	1.5448	Tartu	1.0524	1.0526
Hefei	1.3915	1.3961	Olympia	1.3200	1.3209	S. Peters.	1.1232	1.1232
Djelfa	2.1635	2.1636	Nantes	1.4477	1.4481	Lerwick	0.8367	0.8381
Alburq.	2.2533	2.2546	Budapest	1.2772	1.2811	Helsinki	1.0562	1.0562

- 399 (i) The present model can be considered validated, as these deviations are  
400 not greater than 0.35%.
- 401 (ii) As regards the rate of improvement in annual irradiation, for locations  
402 with  $\lambda < 45^\circ$ , it is up to 0.34%, whereas for  $\lambda \geq 45^\circ$ , the increase is up  
403 to 0.35% in Budapest (nr. 26).
- 404 (iii) Our main remark is that there are many locations for which the dif-  
405 ference between our optimum tilt angle and Jacobson's formula can be  
406 large (by which we mean larger than  $5^\circ$ ); this stresses the importance  
407 of using a method which takes into account the meteorological features  
408 of each place. Notice, for example, Hefei (nr. 11), where our estimate  
409 is 21.6, Jacobson's is 27.5.

#### 410 3.4. Step 4. Racking systems with solar tracker

411 We now study racking systems with solar tracker, whose orientation is  
412 continuously updated. These are classified according to their axes of motion  
413 (either two or one, and the latter depend on their orientation). Table 5 sum-  
414 marizes the different types and the formulas for their tilt and azimuth angles,  
415 following (with a different notation for the polar axis case) [12]. Finally, Ta-  
416 ble 6 contains the estimated values of total annual irradiation (MWh/m<sup>2</sup>)  
417 for each of these systems.

Table 5. Parameters for the types of solar tracker [12].

Tracker	Tilt angle	Surface azimuth angle
Dual-axis	$\theta_z$	$\gamma_s$
Polar axis	$\arccos(\cos \omega \cos \lambda)$	$\gamma = \gamma^*$ if $ \omega  < 90^\circ$
		$\gamma = -180^\circ - \gamma^*$ if $\omega < 90^\circ$
		$\gamma = 180^\circ - \gamma^*$ if $\omega > 90^\circ$
		$\gamma^* = \text{sign}(\omega) \arccos \frac{1}{\sqrt{1 + \frac{\tan^2 \omega}{\sin^2 \lambda}}}$
N-S axis	$\arctan(\tan \theta_z  \cos(\gamma - \gamma_s) )$	$90^\circ (\gamma_s > 0)$ or $-90^\circ (\gamma_s \leq 0)$
E-W axis	$\arctan(\tan \theta_z  \cos \gamma_s )$	$0^\circ ( \gamma_s  < 90^\circ)$ or $180^\circ ( \gamma_s  \geq 90^\circ)$

### 418 3.5. Step 5. Efficacy assessment

419 We evaluate the efficacy of each racking system in relation to the best one  
 420 (dual-axis tracker) in two aspects: the relative loss of energy production and  
 421 the levelized cost of the electrical energy (LCOE) produced. The trackers we  
 422 consider are: (a) single axis with Polar tracker, (b) with North-South axis,  
 423 (c) with East-West axis, (d) no tracker with daily update, (e) no tracker with  
 424 monthly update, and (f) no tracker with constant tilt. Whenever an \* appears  
 425 in any of the formulas below, it should be replaced with the corresponding  
 426 type.

#### 427 3.5.1. Step 5.1 Energy loss ratio

428 We just compute the difference between the energy absorbed by the spe-  
 429 cific system under study and the dual-axis tracker, as a % of energy:

$$430 \quad \text{Energy loss} = \frac{H_* - H_{2-axis}}{H_{2-axis}} \cdot 100 \quad (16)$$

431 Where the subindex \* stands, as above, for the corresponding tracker (Polar,  
 432 North-South, etc.).

#### 433 3.5.2. Step 5.2. LCOE

434 The Levelized Cost of Electrical Energy (LCOE) is a standardized value  
 435 (USD/kWh), defined as the ratio between the life-cycle cost of the PV sys-  
 436 tem and the energy produced during its whole operative life. The following

Table 6. Estimated annual irradiation for systems with solar tracker (MWh/m<sup>2</sup>).

City	Dual-axis	Polar-axis	NS-Single	EW-Single
Medellin	2.1908	2.1371	2.1340	1.8968
Colombo	2.4670	2.4033	2.3951	2.1015
Bangkok	2.2366	2.1788	2.1505	1.9543
Dakar	2.7499	2.6682	2.6310	2.3114
Morelia	2.8536	2.7608	2.6826	2.3143
El Paso	2.1120	2.0552	2.0203	1.8221
Karachi	2.7917	2.7039	2.5880	2.3567
Delhi	2.4339	2.3627	2.2453	2.0798
New Orleans	2.2721	2.1997	2.0893	1.9186
Cairo	2.9540	2.8585	2.7238	2.4161
Hefei	1.6049	1.5602	1.5099	1.4374
Djelfa	2.8689	2.7704	2.5916	2.3150
Alburquerque	3.1041	2.9949	2.7713	2.4364
Handan	1.7688	1.7130	1.6163	1.5614
Desert Rock	3.2269	3.1144	2.8671	2.5185
Almeria	2.7936	2.6998	2.5004	2.2521
Madrid	2.5898	2.5007	2.3029	2.0891
New York	1.9769	1.9093	1.7595	1.6695
Rock Springs	1.7752	1.7160	1.6066	1.4958
Chicago	1.9324	1.8675	1.7436	1.6118
Rome	2.3314	2.2549	2.0890	1.9021
Toronto	1.8004	1.7389	1.6216	1.5166
San Marino	1.9685	1.9003	1.7716	1.6307
Olympia	1.6575	1.5985	1.4847	1.3867
Nantes	1.8539	1.7905	1.6165	1.5339
Budapest	1.5574	1.5038	1.4231	1.3256
Seattle	1.7561	1.6938	1.5574	1.4542
Freiburg	1.7819	1.7214	1.5554	1.4638
Wien	1.6773	1.6186	1.4971	1.4059
Valentia	1.2569	1.2054	1.1257	1.0970
Saskatoon	1.8407	1.7695	1.5747	1.4944
Quebec	1.4662	1.4075	1.2742	1.2290
Berlin	1.4581	1.4028	1.3121	1.2366
Hamburg	1.4950	1.4392	1.3028	1.2361
Alberta	1.7468	1.6761	1.4693	1.4186
Tartu	1.3316	1.2714	1.1590	1.1166
S. Petersbutg	1.4877	1.4274	1.2830	1.1982
Lerwick	1.0587	1.0094	0.8975	0.9254
Helsinki	1.3824	1.3203	1.1926	1.1292

437 definition is given in [67]:

$$438 \quad LCOE = \frac{\sum_{i=0}^I \left[ C_i / (1 + r)^i \right]}{\sum_{i=0}^I \left[ E_i / (1 + r)^i \right]} \quad (17)$$

439 where, for each year  $i$ ,  $C_i$  is the net cost (USD) of the project in that year,  
 440  $E_i$  is the total energy output (in that year, in kWh),  $I$  is the lifetime of the  
 441 project (years) and  $r$  the discount rate. This  $E_i$  can be computed, for PV  
 442 systems, as

$$443 \quad E_i = S_i \cdot \eta \cdot (1 - d)^i \quad (18)$$

444 where  $S_i$  is the availability of solar resources in year  $i$  (kWh),  $\eta$  is the per-  
 445 formance factor, and  $d$  is the annual degradation rate. Thus, the LCOE  
 446 gathers in a single value the initial investment cost, the operation and main-  
 447 tenance costs, the interest expenditure if financed, and, on the other hand,  
 448 the energetic output.

449 Obviously, the LCOE depends on site-specific parameters as power capaci-  
 450 ty, PV technology, location... In order to provide a reasonable assessment,  
 451 we are going to assume from now on, as elsewhere in the literature, the  
 452 following:

453 (i) *Initial investment cost.* As explained in the introduction, dual axis  
 454 tracking systems require a greater initial investment than single-axis  
 455 or fixed systems, with a premium of 40 – 50% over fixed systems, and  
 456 20 – 25% over single-axis ones [8]. In this paper, we assume respective  
 457 premiums of 50% and 25%.

458 (ii) *Operation and maintenance costs.* Despite the lack of standardization  
 459 [10] for this value, the National Renewable Energy Laboratory recom-  
 460 mends assuming an annual cost of 0.5% of the total initial cost for  
 461 large systems, and 1% for small ones. Moreover, Mortensen [68] sug-  
 462 gests that operation and maintenance costs with tracking systems are  
 463 double those of fixed-tilt ones. We are going to assume 0.5% of the  
 464 initial investment for systems with tracking, and 0.25% for systems  
 465 without.

466 (iii) *Interest costs (financing).* We are not taking into account this value,  
 467 as it is outside the scope of any control.

- 468 (iv) *Discount rate.* For the same reasons, we are not going to take into  
 469 account this value (i.e.  $r = 0$ ), as these are country- and time-specific.
- 470 (v) *Total electrical energy output.* This value is directly proportional to the  
 471 availability of solar resources at each location. We consider the same  
 472 performance factor and degradation rate for all the systems.
- 473 (vi) *Project lifetime.* We take a fixed value of 20 years [67].

474 From the considerations above, it follows that location is quite relevant  
 475 in the computation of the LCOE. We are going to use the following ratio to  
 476 compare the LCOE values for single-axis and fixed-tilt systems to two-axis  
 477 systems ( $LCOE_{2-axis}$ ):

$$478 \quad \eta_{LCOE} = \frac{LCOE_*}{LCOE_{2-axis}} \quad (19)$$

479 where, as above,  $*$  is one of the different tracking systems we are comparing.  
 480 Notice that an  $\eta_{LCOE}$  value greater than 1 implies that the corresponding  
 481 tracking system is *less* efficient than the dual-axis system.

#### 482 4. Results and discussion

483 Based on the methodology presented above, the Computer Algebra Sys-  
 484 tem Mathematica<sup>©</sup> was used for computing the total annual irradiation at  
 485 39 sites covering a large part of the Northern Hemisphere, as well as the total  
 486 energy produced by the different PV systems with or without solar tracking,  
 487 with optimum tilt angles. The PVGIS [70] database was used to obtain the  
 488 irradiation data with which to compute the estimated irradiance. The LCOE  
 489 is the metric used to analyze their efficiency. The remainder of this section  
 490 contains the outputs of our computations and the comparison of each system  
 491 with the best one, the dual-axis tracker.

492 For a specific location, we start by collecting the satellite estimations of  
 493 monthly-averaged global and diffuse solar irradiances received on a horizon-  
 494 tal surface. We use the publicly available PVGIS database [70], but any  
 495 other source is equivalent. From these monthly values, we compute, using  
 496 Fourier analysis and the classic clear-sky beam and diffuse irradiation models  
 497 [36] (in this paper we apply the Hottel and Liu Jordan models, respectively),  
 498 hourly distributions for the beam and diffuse solar irradiances. By integra-  
 499 tion, taking into account that  $\beta$  can be updated hourly, daily, monthly or be

500 constant throughout the year, we obtain the total irradiation for each day of  
 501 the year and the different tilt upgrade frequencies. A main advantage of our  
 502 methodology is that it takes into account the main environmental conditions  
 503 of the site.

#### 504 4.1. Evaluation of energy losses

505 In this section we calculate the losses in produced energy of the different  
 506 systems with respect to the dual-axis tracker. Fig. 10 contains this compar-  
 507 ison using Eq. (16).

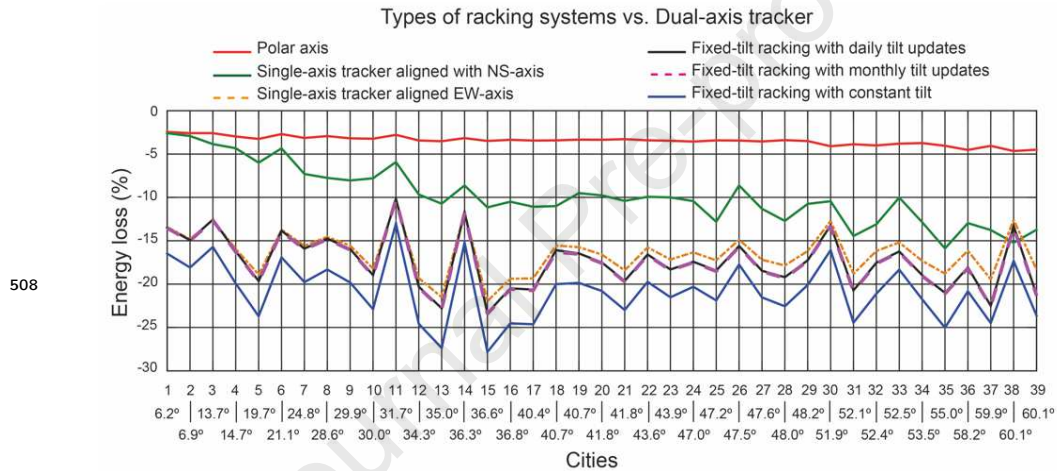


Fig. 10. Ratio of energy loss with respect to the dual-axis tracker.  
 Notice that the daily and monthly plots overlap.

509 Fig. 10 suggests the following conclusions:

- 510 (i) Obviously, dual-axis tracker systems yield the best performance every-  
 511 where.
- 512 (ii) The maximum loss of absorbed energy for the polar axis tracker is  
 513 3.46% for locations with  $\lambda < 45^\circ$ , and 4.65% for locations with  $\lambda \geq 45^\circ$ .
- 514 (iii) For North-South aligned axis trackers, the maximum losses are 11.15%  
 515 for  $\lambda < 45^\circ$  and 15.88% for  $\lambda \geq 45^\circ$ .
- 516 (iv) For East-West aligned axis trackers, these maxima are 21.95% and  
 517 19.45%, respectively.

518 (v) The least efficient systems is the constant-tilt one, with maximum (rel-  
 519 ative) loss of 27.82% at Desert Rock (nr. 15).

520 One of the most striking results (in our view) is the surprisingly good  
 521 results obtained using the system without tracker with monthly tilt update.  
 522 Notice also, from Fig. 10 that:

523 (i) Updating the tilt angle daily is only marginally better than doing so  
 524 monthly.

525 (ii) The spread of this improvement is the interval 0.07% to 0.14% (Bangkok  
 526 (nr. 3) and Desert Rock (nr. 15)), respectively.

527 (iii) The reason for this small difference can be glimpsed in Fig. 11, which  
 528 plots the daily absolute differences in irradiation between the daily and  
 529 the monthly update method, in the specific case of Almeria (nr. 16).  
 530 There is only a significant difference on the first days of each month, and  
 531 this does not reach even 1% (less than 50Wh/m<sup>2</sup> of daily irradiation).

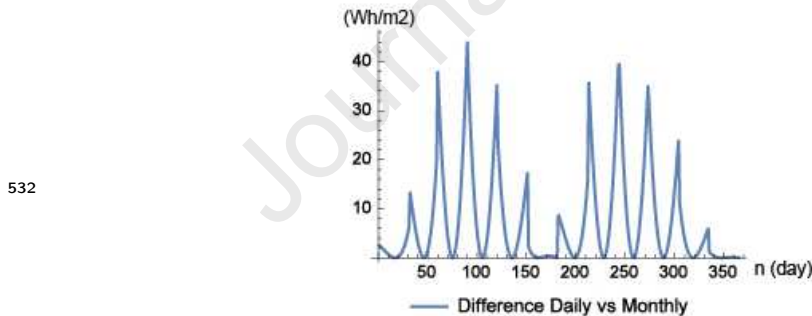


Fig. 11. Difference in irradiation between daily and monthly tilt updates.

533 On the other hand, the improvement in energy production, with respect  
 534 to the constant-tilt system, if the is updated monthly, is between 2.53% (St.  
 535 Petersbutg, nr. 37) and 6.16% (Albuquerque, nr. 13).

536 Fig. 12 shows the total daily solar irradiation harvested throughout the  
 537 year in Almeria (nr. 16), using single axis trackers with East-West axis,  
 538 and trackerless systems with daily update and with constant tilt. Clearly,  
 539 the main difference takes place during the Summer and, remarkably, the first  
 540 two systems give essentially the same values except for the central days of the

541 year. Constant-tilt systems show a very good efficiency near the equinoxes  
 542 but also great losses at other times.

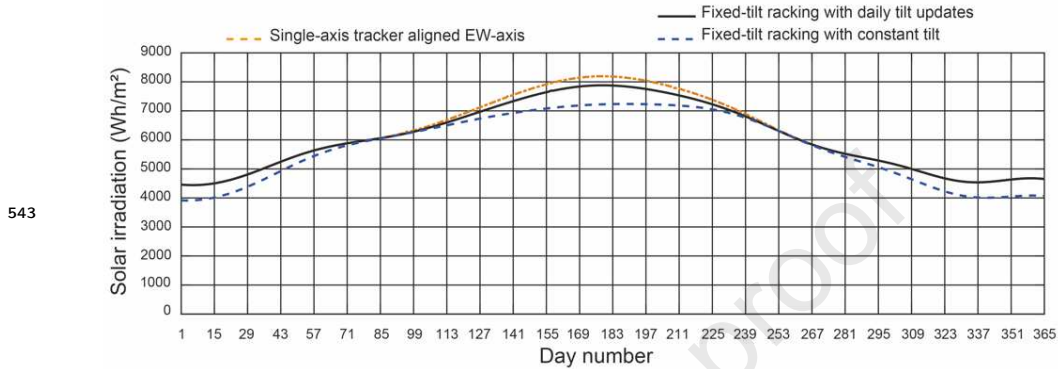


Fig. 12. Daily irradiation in Almeria (nr. 16).

544 *4.2. Evaluation of the systems with respect to the LCOE*

545 We now compare the LCOE of all the systems, taking as baseline the most  
 546 energy-efficient (the dual-axis tracker), by computing the ratio between the  
 547 LCOE of each of the others and this one. The summary results are shown  
 548 in Fig. 13, for which Eq. (19) has been used.

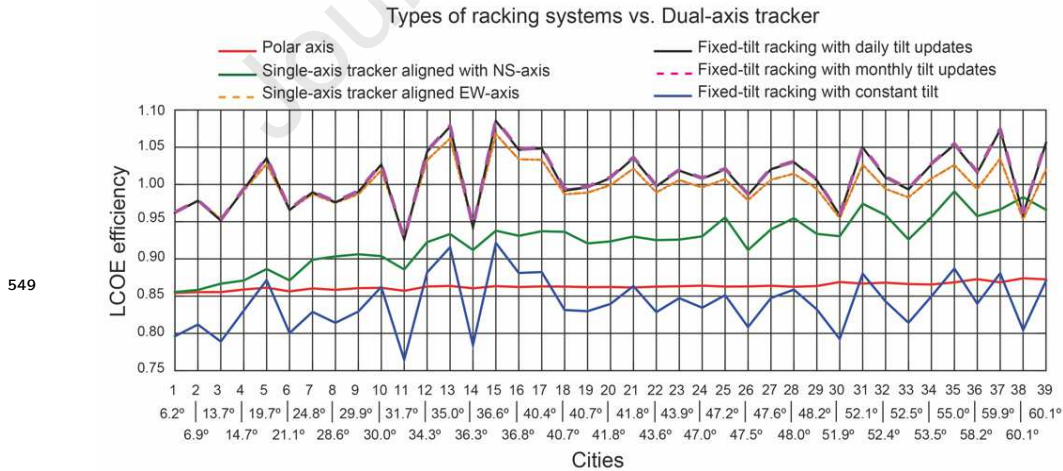


Fig. 13. LCOE efficiency with respect to the dual-axis tracker.  
 Notice that the daily and monthly plots overlap.

550 The following conclusions can be inferred from Fig. 13:

- 551 (i) The most efficient system with respect to LCOE is the one without  
 552 solar tracker with constant tilt (no update whatsoever). Despite being  
 553 the one which generates the least energy, it also requires the least initial  
 554 investment. The ratio of LCOE with respect to the dual-axis tracker  
 555 varies between 0.76 (Hefei, nr. 11) and 0.91 (Albuquerque, nr. 13).
- 556 (ii) The single-axis system with polar axis shows a good LCOE efficiency,  
 557 and notably, its ratio with respect to the dual-axis tracker is essentially  
 558 the same for all latitudes (between 0.85 and 0.87).
- 559 (iii) The N-S oriented single-axis system has also a good LCOE efficiency,  
 560 but its improvement ratio depends greatly on the latitude: between  
 561 0.85 (Medellin, nr. 1) and 0.99 (Alberta, nr. 35).
- 562 (iv) Single-axis systems with East-West alignment, and systems without  
 563 tracker but daily or monthly updates are the worst in terms of this  
 564 metric. They are the ones producing the least energy (except for the  
 565 constant tilt) and their initial investment does not make up for that  
 566 loss.

567 The sensitivity of the model is measured as the influence of the initial  
 568 investment cost on LCOE. Notice that the initial investment cost of the dual-  
 569 axis tracker is greater than the rest of the systems. We are going to use the  
 570 initial investment costs specified in Section 3.5: there is a premium in the  
 571 dual tracker of 40–50% over fixed systems and a of 20–25% over single-axis  
 572 ones [8]. Fig. 14 illustrate our sensitivity analysis for Almeria (nr. 16). The  
 573 following conclusions can be inferred:

574

- 575 (i) Regardless of the initial investment cost, the polar axis, the single-axis  
 576 tracker aligned with NS-axis and the fixed-tilt racking with constant  
 577 tilt have always a good LCOE.
- 578 (ii) The single-axis tracker aligned with EW-axis, the fixed-tilt racking with  
 579 daily tilt updates, and the fixed-tilt racking with monthly tilt updates  
 580 have always a bad LCOE.
- 581 (iii) The best LCOE is reached when the initial investment of the dual-axis  
 582 system is minimal with respect to the single-axis one, and when the  
 583 initial investment of the dual axis-system is maximal with respect to  
 584 the fixed system.

- 585 (iv) The worst LCOE happens when the initial investment of the dual-axis  
 586 system is maximal with respect to the single-axis, and when the initial  
 587 investment of the dual-axis system is minimal with respect to the fixed  
 588 one.

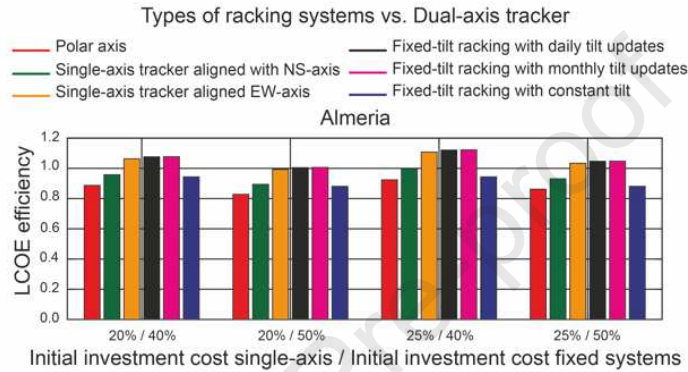


Fig. 14. Sensitivity analysis of LCOE with respect to the dual-axis tracker in Almeria.

## 589 5. Conclusions

590 We have carried out a comparative study of the efficiency of different  
 591 racking systems of photovoltaic power systems in 39 locations in the North  
 592 Hemisphere covering a wide range of latitudes.

593 In order to do so, a new methodology for computing the optimum tilt an-  
 594 gles for racking systems without solar tracker (either with fixed tilt or allowing  
 595 daily/monthly updates) is developed, which allows us to compare those sys-  
 596 tems to the ones with solar tracker (be it dual-axis tracker, polar axis racker,  
 597 single-axis tracker aligned with North-South or East-West axis), taking into  
 598 account both the geographical and the meteorological conditions of the sites.

599 The proposed methodology requires, apart from the latitude and altitude  
 600 of the site, just the knowledge of the 12 values of daily averages of monthly  
 601 solar irradiation (beam and diffuse). We validate it for systems with daily  
 602 update by comparing our results to the values obtained using Duffie's formula  
 603 with daily update, and find our values within an acceptable range (deviations  
 604 of less than 2.5% in annual energy production). For systems with constant

605 tilt, we compare method our results with Jacobson's (14), and find a very  
 606 good agreement (deviations less than 0.35%).

607 Specifically, we study 39 cities which cover all the latitudes in the North-  
 608 ern Hemisphere and a large spectrum of longitudes. Using Mathematica<sup>®</sup>,  
 609 we compute the optimum tilts angles for each day, month and year for sys-  
 610 tems without tracker. We also estimate the total solar irradiation for each of  
 611 the possible tracking systems, compare them and compare their respective  
 612 LCOE. In summary, our analysis yields the following conclusions:

- 613 (i) Obviously, dual-axis tracker systems are the most energy productive.  
 614 However, they have also the worst LCOE (among those with tracker).
- 615 (ii) For polar-axis systems, the maximum loss of absorbed energy (for the  
 616 locations studied) is 3.46% (always with respect to the dual-axis sys-  
 617 tem) for latitudes less than  $45^\circ$  and 4.65% for  $\lambda \geq 45^\circ$ . These have a  
 618 good LCOE.
- 619 (iii) For North-South oriented systems, the loss of absorbed energy is at  
 620 most 11.15% for places with  $\lambda < 45^\circ$  and 15.88 for  $\lambda \geq 45^\circ$ . The  
 621 LCOE is worse than for the polar-axis systems.
- 622 (iv) For East-West oriented systems, the loss of absorbed energy is at most  
 623 21.95% for  $\lambda < 45^\circ$  and 19.45% for  $\lambda \geq 45^\circ$ . The LCOE of these  
 624 systems is even worse than for North-South oriented ones.
- 625 (v) The energy loss for fixed-tilt systems with daily update with respect to  
 626 East-West oriented systems is at most 3.76%.
- 627 (vi) The difference in energy absorption between fixed-tilt systems with  
 628 daily update and with monthly update is negligible: this is a remarkable  
 629 property which may have important budgetary consequences (both in  
 630 design and maintenance costs).
- 631 (vii) In the absence of solar tracker, a system with constant tilt (no update)  
 632 is consistently and significantly worse than one with monthly updates,  
 633 with typical losses around 3.5% and even reaching 6.1%. However, the  
 634 LCOE is much better (up to 20% better).

635 We consider that our methodology and its analysis can serve to make opti-  
 636 mal decisions in the choice of racking systems of photovoltaic power systems,

637 yielding significant benefits from the point of view of total energy absorption  
638 and budget optimization.

### 639 **Acknowledgments**

640 We wish to thank Gonvarri Solar Steel [8] for his contribution in this  
641 paper.

- 642 [1] BP, Statistical Review of World Energy; 2019, 68th edition,  
643 Available from: [https://www.bp.com/content/dam/bp/business-](https://www.bp.com/content/dam/bp/business-sites/en/global/corporate/pdfs/energy-economics/statistical-review/bp-stats-review-2019-full-report.pdf)  
644 [sites/en/global/corporate/pdfs/energy-economics/statistical-](https://www.bp.com/content/dam/bp/business-sites/en/global/corporate/pdfs/energy-economics/statistical-review/bp-stats-review-2019-full-report.pdf)  
645 [review/bp-stats-review-2019-full-report.pdf](https://www.bp.com/content/dam/bp/business-sites/en/global/corporate/pdfs/energy-economics/statistical-review/bp-stats-review-2019-full-report.pdf), accessed on 23 December  
646 2020.
- 647 [2] G. Liu, M.G. Rasul, M.T.O. Amanullah, M.M.K. Khan, Techno-  
648 economic simulation and optimization of residential grid-connected PV  
649 system for the Queensland climate, *Renewable Energy* 45 (2012) 146–  
650 155.
- 651 [3] S. Yilmaz, H.R. Ozcalik, S. Kesler, F. Dincer, B. Yelmen, The analy-  
652 sis of different PV power systems for the determination of optimal PV  
653 panels and system installation—A casestudy in Kahramanmaras, Turkey,  
654 *Renewable and Sustainable Energy Reviews* 52 (2015) 1015–1024.
- 655 [4] IEA, Trends in photovoltaic applications: 2019. International Renew-  
656 able Energy Agency. Available from: [https://www.comitesolar.cl/wp-](https://www.comitesolar.cl/wp-content/uploads/2019/12/Iea-pvps_report_2019.pdf)  
657 [content/uploads/2019/12/Iea-pvps\\_report\\_2019.pdf](https://www.comitesolar.cl/wp-content/uploads/2019/12/Iea-pvps_report_2019.pdf), accessed on 23  
658 December 2020.
- 659 [5] IRENA, Future of solar photovoltaic: Deployment, investment, tech-  
660 nology, grid integration and socio-economic aspects; 2019. International  
661 Renewable Energy Agency. Available from: [https://irena.org/-](https://irena.org/-/media/Files/IRENA/Agency/Publication/2019/Nov/IRENA_Future_of_Solar_PV_2019.pdf)  
662 [/media/Files/IRENA/Agency/Publication/2019/Nov/IRENA\\_](https://irena.org/-/media/Files/IRENA/Agency/Publication/2019/Nov/IRENA_Future_of_Solar_PV_2019.pdf)  
663 [\\_Fu-](https://irena.org/-/media/Files/IRENA/Agency/Publication/2019/Nov/IRENA_Future_of_Solar_PV_2019.pdf)  
664 [ture\\_of\\_](https://irena.org/-/media/Files/IRENA/Agency/Publication/2019/Nov/IRENA_Future_of_Solar_PV_2019.pdf)  
[Solar\\_PV\\_2019.pdf](https://irena.org/-/media/Files/IRENA/Agency/Publication/2019/Nov/IRENA_Future_of_Solar_PV_2019.pdf), accessed on 23 December 2020.
- 665 [6] O. Savu, Good practice: Photovoltaic Park Ciurbesti - Miroslava,  
666 European Union, [[https://www.interregeurope.eu/policylearning/good-](https://www.interregeurope.eu/policylearning/good-practices/item/886/photovoltaic-park-ciurbesti-miroslava-com/)  
667 [practices/item/886/photovoltaic-park-ciurbesti-miroslava-com/](https://www.interregeurope.eu/policylearning/good-practices/item/886/photovoltaic-park-ciurbesti-miroslava-com/)],  
668 accessed on 23 December 2020.

- 669 [7] R. Srivastava, A.N. Tiwari, V.K. Giri, An overview on performance of  
670 PV plants commissioned at different places in the world, *Energy for*  
671 *Sustainable Development* 54 (2020) 51-59.
- 672 [8] Gonvarri Solar Steel, <https://www.gsolarsteel.com/>, accessed on 23 De-  
673 cember 2020.
- 674 [9] Kiewit, [https://www.kiewit.com/plant-insider/current-issue/](https://www.kiewit.com/plant-insider/current-issue/fixed-tilt-vs-axis-tracker-solar-panels/)  
675 [fixed-tilt-vs-axis-tracker-solar-panels/](https://www.kiewit.com/plant-insider/current-issue/fixed-tilt-vs-axis-tracker-solar-panels/) accessed on 23 December 2020.
- 676 [10] D.L. Talavera, Emilio Muñoz-Cerón, J.P. Ferrer-Rodríguez, P.J. Pérez-  
677 Higuera, Assessment of cost-competitiveness and profitability of fixed  
678 and tracking photovoltaic systems: The case of five specific sites, *Re-*  
679 *newable Energy* 134 (2019) 902-913.
- 680 [11] NREL, Best practices for operation and maintenance of  
681 photovoltaic and energy storage systems, 3rd Edition.  
682 Golden, CO: National Renewable Energy Laboratory, 2018.  
683 <https://www.nrel.gov/docs/fy19osti/73822.pdf>. (Accessed 23 De-  
684 cember 2020).
- 685 [12] J.A. Duffie, W.A. Beckman, *Solar Engineering of Thermal Processes*, 4  
686 ed. New York: John Wiley & Sons; 2013.
- 687 [13] A.Z. Hafez, A. Soliman, K.A. El-Metwally, I.M. Ismail, Tilt and az-  
688 imuth angles in solar energy applications – A review, *Renewable and*  
689 *Sustainable Energy Reviews* 77 (2017) 147–168.
- 690 [14] N. Bailek, K. Bouchouicha, N. Aoun, M. EL-Shimy, B. Jamil, A.  
691 Mostafaeipour, Optimized fixed tilt for incident solar energy maximiza-  
692 tion on flat surfaces located in the Algerian Big South, *Sustainable En-*  
693 *ergy Technologies and Assessments* 28 (2018) 96–102.
- 694 [15] M. Jiménez-Torres, C. Rus-Casas, L. Lemus-Zúñiga, L. Hontoria, The  
695 importance of accurate solar data for designing solar photovoltaic  
696 systems—case studies in Spain, *Sustainability* 9 (2017) 247-259.
- 697 [16] H. Darhmaoui, D. Lahjouji, Latitude based model for tilt angle optimiza-  
698 tion for solar collectors in the Mediterranean region, *Energy Procedia*  
699 42 (2013) 426–435.

- 700 [17] M.A. Danandeh, S.M. Mousavi, Solar irradiance estimation models and  
701 optimum tilt angle approaches: A comparative study, *Renewable and*  
702 *Sustainable Energy Reviews* 92 (2018) 319–330.
- 703 [18] RENEWIT, RenewIT Project; 2016. Available from:  
704 <http://www.renewit-project.eu/RenewIT> tool: Advanced concepts  
705 and tools for renewable energy supply of IT Data Centres/, accessed on  
706 23 December 2020.
- 707 [19] A. Luque, S. Hegedus, *Handbook of Photovoltaic Science and Engineer-*  
708 *ing*, 1 ed. Chichester: John Wiley & Sons; 2003.
- 709 [20] T.P. Chang, The Sun’s apparent position and the optimal tilt angle of  
710 a solar collector in the northern hemisphere, *Solar Energy* 83 (2009)  
711 1274–1284.
- 712 [21] P. Talebizadeh, M.A. Mehrabian, M. Abdolzadeh, Determination of op-  
713 timum slope angles of solar collectors based on new correlations, *Energy*  
714 *Sources Part A* 33 (2011) 1567-1580.
- 715 [22] M.Z. Jacobson, V. Jadhav, World estimates of PV optimal tilt angles  
716 and ratios of sunlight incident upon tilted and tracked PV panels relative  
717 to horizontal panels, *Solar Energy* 169 (2018) 55-66.
- 718 [23] A. Barbón, C. Bayón-Cueli, L. Bayón, C. Rodríguez-Suanzes, Analy-  
719 sis of the tilt and azimuth angles of photovoltaic systems in non-ideal  
720 positions for urban applications, *Applied Energy* (2021) in press.
- 721 [24] A. Ullah, H. Imran, Z. Maqsood, N.Z. Butt, Investigation of optimal  
722 tilt angles and effects of soiling on PV energy production in Pakistan,  
723 *Renewable Energy* 139 (2019) 830-843.
- 724 [25] NREL, National, Solar Radiation Data Base; 2014. Available from:  
725 [http://rredc.nrel.gov/solar/old\\_data/nsrdb/](http://rredc.nrel.gov/solar/old_data/nsrdb/), accessed on 23 December  
726 2020.
- 727 [26] ESMAP, Solar Radiation Measurement Data; 2016. Available from:  
728 [https://energydata.info/dataset/pakistan-solar-measurement-wbg-](https://energydata.info/dataset/pakistan-solar-measurement-wbg-esmap/resource/3d0dd820-b2c3-4946-a032-c7a2a4c2bd7b)  
729 [esmap/resource/3d0dd820-b2c3-4946-a032-c7a2a4c2bd7b](https://energydata.info/dataset/pakistan-solar-measurement-wbg-esmap/resource/3d0dd820-b2c3-4946-a032-c7a2a4c2bd7b), accessed on  
730 23 December 2020.

- 731 [27] Y. Lv, P. Si, X. Rong, J. Yan, Y. Feng, X. Zhu, Determination of op-  
732 timum tilt angle and orientation for solar collectors based on effective  
733 solar heat collection, *Applied Energy* 219 (2018) 11-19.
- 734 [28] CDCCMA, Climatic Data Center of China Meteorological Administra-  
735 tion, Tsinghua University. Meteorological Data Set for China Building  
736 Thermal Environment Analysis (in Chinese). 1st ed. Beijing: China Ar-  
737 chitecture & Building Press; 2005.
- 738 [29] F. Jafarkazemi, S.A. Saadabadi, Optimum tilt angle and orientation of  
739 solar surfaces in Abu Dhabi, UAE, *Renewable Energy* 56 (2013) 44-49.
- 740 [30] M.D. Islam, I. Kubo, M. Ohadi, AA.. Alili, Measurement of solar energy  
741 radiation in Abu Dhabi, UAE, *Renewable Energy* 86 (2009) 511-515.
- 742 [31] K. Skeiker, Optimum tilt angle and orientation for solar collectors in  
743 Syria, *Energy Conversion and Management* 50 (2009) 2439-2448.
- 744 [32] A.E.S.A. Nafeh, Evaluation of the optimum tilts of a PV array using  
745 maximum global insolation technique, *International Journal of Numerical  
746 Modeling Electronic Networks Devices and Fields* 17 (2004) 385-395.
- 747 [33] N. Nijegorodov, K.R.S. Devan, P.K. Jain , S. Carlsson, Atmospheric  
748 transmittance models and an analytical method to predict the optimum  
749 slope on an absorber plate, variously orientated at any latitude, *Renew-  
750 able Energy* 4 (1994) 529-543.
- 751 [34] H. Gunerhan, A. Hepbasli, Determination of the optimum tilt angle of  
752 solar collectors for building applications, *Building and Environment* 42  
753 (2007) 779-783.
- 754 [35] UN, World Population Prospects 2019; 2019. United Nations. Available  
755 from: <https://population.un.org/wpp/>, accessed on 23 December 2020.
- 756 [36] A. Barbón, P. Fortuny Ayuso, L. Bayón, J.A. Fernández-Rubiera, Pre-  
757 dicting beam and diffuse horizontal irradiance using Fourier expansions,  
758 *Renewable Energy* 154 (2020) 46-57.
- 759 [37] ASHRAE Handbook: HVAC applications. Chapter 32. Atlanta (GA):  
760 ASHRAE, 1999.

- 761 [38] C. Vernay, S. Pitaval, P. Blanc, Review of satellite-based surface solar ir-  
762 radiation databases for the engineering, the financing and the operating  
763 of photovoltaic systems, *Energy Procedia* 57 (2014) 1383 – 1391.
- 764 [39] A. Angström, Solar and terrestrial radiation, *Quarterly Journal of Royal*  
765 *Meteorological Society* 50 (1924) 121–125.
- 766 [40] M. Paulescu, L. Fara, E. Tulcan-Paulescu, Models for obtaining daily  
767 global solar irradiation from air temperature data, *Atmospheric Re-*  
768 *search* 79 (2006) 227–240.
- 769 [41] H.C. Hottel, A simple model for estimating the transmittance of direct  
770 solar radiation through clear atmosphere, *Solar Energy* 18 (1976) 129-  
771 134.
- 772 [42] B.Y.H. Liu, R.C. Jordan, The interrelationship and characteristic distri-  
773 bution of direct, diffuse and total solar radiation, *Solar Energy* 4 (1960)  
774 1-19.
- 775 [43] WRDC. World radiation data Centre, Available on line at 2020,  
776 <http://wrdc.mgo.rssi.ru/>.
- 777 [44] D.S. Moore, W.I. Notz, M. A. Flinger, *The basic practice of statistics*,  
778 sixth ed. W. H. Freeman, New York, 2013.
- 779 [45] B.Y.H. Liu, R.C. Jordan, The long-term average performance of flat-  
780 plate solar energy collectors, *Solar Energy* 7 (1963) 53-74.
- 781 [46] T. Muneer, *Solar radiation and day light models*. 1 ed Oxford: Elsevier;  
782 2004.
- 783 [47] K.N. Shukla, S. Rangnekar, K. Sudhakar, Comparative study of isotropic  
784 and anisotropic sky models to estimate solar radiation incident on tilted  
785 surface: A case study for Bhopal, India, *Energy Reports* 1 (2015) 96–  
786 103.
- 787 [48] P.S. Koronakis, On the choice of angle of tilt for south facing solar  
788 collectors in Athens Basin Area, *Solar Energy* 36 (1986) 217–225.
- 789 [49] V. Badescu, 3D isotropic approximation for solar diffuse irradiance on  
790 tilted surfaces, *Renewable Energy* 26 (2002) 221–233.

- 791 [50] Y.Q. Tian, R.J. Davies-Colley, P. Gong, B.W. Thorrold, Estimating  
792 solar radiation on slopes of arbitrary aspect, *Agricultural and Forest*  
793 *Meteorology* 109 (2001) 67–74.
- 794 [51] J.W. Bugler, The determination of hourly insolation on an inclined plane  
795 using a diffuse irradiance model based on hourly measured global hori-  
796 zontal insolation, *Solar Energy* 19 (1977) 477–491.
- 797 [52] C.C.Y. Ma, M. Iqbal, Statistical comparison of models for estimating  
798 solar radiation on inclined surfaces, *Solar Energy* 31 (1983) 313–317.
- 799 [53] M. Iqbal, *An introduction to solar radiation*. 1 ed New York: Academic  
800 Press Inc.; 1983.
- 801 [54] R. Perez, R. Seals, P. Ineichen, R. Stewart, D. Menicucci, A new sim-  
802 plified version of the Perez diffuse irradiance model for tilted surfaces,  
803 *Solar Energy* 39 (3) (1987) 221–231.
- 804 [55] R. Perez, R. Seals, J. Michalsky, All weather model for sky luminance  
805 distribution - Preliminary configuration and validation, *Solar Energy* 50  
806 (3) (1993) 235–245.
- 807 [56] R.C. Temps, K.L. Coulson, Solar radiation incident upon slopes of dif-  
808 ferent orientations, *Solar Energy* 19 (1977) 179–184.
- 809 [57] T.M. Klucher, Evaluation of models to predict insolation on tilted sur-  
810 faces, *Solar Energy* 23 (1979) 111–114.
- 811 [58] D.T. Reindl, W.A. Beckman, J.A. Duffie, Diffuse fraction correlations,  
812 *Solar Energy* 45 (1990) 1–7.
- 813 [59] E.D. Mehleri, P.L. Zervas, H. Sarimveis, J.A. Palyvos, N.C. Markatos,  
814 Determination of the optimal tilt angle and orientation for solar photo-  
815 voltaic arrays, *Renewable Energy* 35 (2010) 2468–2475.
- 816 [60] J.I. Jiménez, Y. Castro-Díez, *National assembly of geophysics and*  
817 *geodesy II* (1986) 805.
- 818 [61] C.K. Pandey, A.K. Katiyar AK, Hourly solar radiation on inclined sur-  
819 faces, *Sustainable Energy Technologies and Assessments* 6 (2014) 86–92.

- 820 [62] G. Fubini, *Opere Scelte Vol. 2. Edizioni Cremonese Roma. Unione*  
821 *Matematica Italiana/CNR* 1958:243-249.
- 822 [63] J. Müller, D. Folini, M. Wild, S. Pfenninger, CMIP-5 models project  
823 photovoltaics are a no-regrets investment in Europe irrespective of cli-  
824 mate change, *Energy* 171 (2019) 135-148.
- 825 [64] H.Z. Al Garni, A. Awasthi, Wright D. Optimal orientation angles for  
826 maximizing energy yield for solar PV in Saudi Arabia, *Renewable En-*  
827 *ergy* 133 (2019) 538-550.
- 828 [65] J. Ascencio-Vásquez, K. Brecl, M. Topič, Methodology of Köppen-  
829 Geiger-Photovoltaic climate classification and implications to worldwide  
830 mapping of PV system performance, *Solar Energy* 191 (2019) 672–685.
- 831 [66] T. Tröndle, S. Pfenninger, J. Lilliestam, Home-made or imported: On  
832 the possibility for renewable electricity autarky on all scales in Europe,  
833 *Energy Strategy Reviews* 26 (2019) 100388.
- 834 [67] K. Branker, M.J.M. Pathak, J.M. Pearce, A review of solar photovoltaic  
835 levelized cost of electricity, *Renewable and Sustainable Energy Reviews*  
836 15 (2011) 4470– 4482.
- 837 [68] J. Mortensen, Factors associated with photovoltaic system costs, Golden  
838 CO: National RENEwable Energy Laboratory, 2001.
- 839 [69] PHOTIUS. [https://photius.com/rankings/2019/economy/central\\_bank](https://photius.com/rankings/2019/economy/central_bank_discount_rate_2019_0.html)  
840 [\\_discount\\_rate\\_2019\\_0.html](https://photius.com/rankings/2019/economy/central_bank_discount_rate_2019_0.html). (Accessed 10 September 2020).
- 841 [70] PVGIS, Joint Research Centre (JRC); 2019. Available from:  
842 [http://re.jrc.ec.europa.eu/pvg\\_tools/en/tools.html#PVP](http://re.jrc.ec.europa.eu/pvg_tools/en/tools.html#PVP), accessed on  
843 23 December 2020.

## Nomenclature

$d$	Annual degradation rate (dimensionless)	$S_i$	Availability of solar resource ( $Wh/m^2$ )
$C_i$	Net cost of the project (USD)	$T$	Solar time ( $h$ )
$E_i$	Total electrical energy output ( $kWh$ )	$T_R$	Sunrise solar time ( $h$ )
$H_t$	Total irradiation on a tilted surface ( $Wh/m^2$ )	$T_S$	Sunset solar time ( $h$ )
$H_t^\beta$	Annual total irradiation for fixed tilt ( $Wh/m^2$ )	$\alpha_S$	Height angle of the Sun ( $rad$ )
$H_t^n$	Annual total irradiation for fixed day ( $Wh/m^2$ )	$\beta$	Tilt angle of photovoltaic panel ( $rad$ )
$H_t^{\beta,m}$	Annual total irradiation for fixed tilt on each month ( $Wh/m^2$ )	$\beta_{opt}^y$	Optimal annual tilt angle ( $rad$ )
$I$	Lifetime of the project ( $years$ )	$\beta_{opt}^d$	Optimal daily tilt angle ( $rad$ )
$I_{bh}$	Beam irradiance on a horizontal surface ( $W/m^2$ )	$\beta_{opt}^m$	Optimal monthly tilt angle ( $rad$ )
$I_{dh}$	Diffuse irradiance on a horizontal surface ( $W/m^2$ )	$\gamma_S$	Azimuth of the Sun ( $rad$ )
LCOE	Levelized cost of the produced electrical energy ( $USD/kWh$ )	$\delta$	Solar declination ( $rad$ )
$I_t$	Total irradiance on a tilted surface ( $W/m^2$ )	$\eta$	Performance factor of PV module (dimensionless)
$n$	Ordinal of the day ( $day$ )	$\eta_{LCOE}$	Levelized cost of the produced electrical energy efficiency (dimensionless)
$r$	Discount rate (dimensionless)	$\theta_i$	Incidence angle ( $rad$ )
		$\theta_z$	Zenith angle of the Sun ( $rad$ )
		$\lambda$	Latitude angle ( $rad$ )
		$\omega$	Hour angle ( $rad$ )
		$\omega_S$	Sunset hour angle ( $rad$ )
		$\omega_S^T$	Sunset hour angle ( $h$ )

**Declaration of interests**

- The authors declare that they have no known competing financial interests or personal relationships that could have appeared to influence the work reported in this paper.
- The authors declare the following financial interests/personal relationships which may be considered as potential competing interests:

Journal Pre-proof